Electronic Supplementary Material (ESI) for Inorganic Chemistry Frontiers.

Electronic Supplementary Information

Anion-driven tetrel bond-induced engineering of lead(II) architectures with *N'*-(1-(2-pyridyl)ethylidene)nicotinohydrazide: Experimental and theoretical findings

Ghodrat Mahmoudi,*[a] Damir A. Safin,*[b] Mariusz P. Mitoraj,*[c] Mojtaba Amini,*[a] Maciej Kubicki,[d] Thomas Doert,[e] Franziska Locherer[e] and Michel Fleck[f]

[a]*Department of Chemistry, Faculty of Science, University of Maragheh, P.O. Box 55181-83111, Maragheh, Iran. E-mail: mahmoudi_ghodrat@yahoo.co.uk, mamini@maragheh.ac.ir*

[b]*Institute of Condensed Matter and Nanosciences, Molecules, Solids and Reactivity (IMCN/MOST), Université catholique de Louvain, Place L. Pasteur 1, 1348 Louvain-la-Neuve, Belgium. E-mail: damir.a.safin@gmail.com*

[c]*Department of Theoretical Chemistry, Faculty of Chemistry, Jagiellonian University, R. Ingardena 3, 30-060 Cracow, Poland. E-mail: mitoraj@chemia.uj.edu.pl*

[d]*Faculty of Chemistry, Adam Mickiewicz University in Poznan, Umultowska 89b, 61-614 Poznan, Poland*

[e]*Department of Chemistry and Food Chemistry, Dresden University of Technology Helmholtzstrasse 10, 01069 Dresden, Germany*

[f]*Institute for Mineralogy and Crystallography, University of Vienna, Althanstrasse 14, 1090 Vienna, Austria*

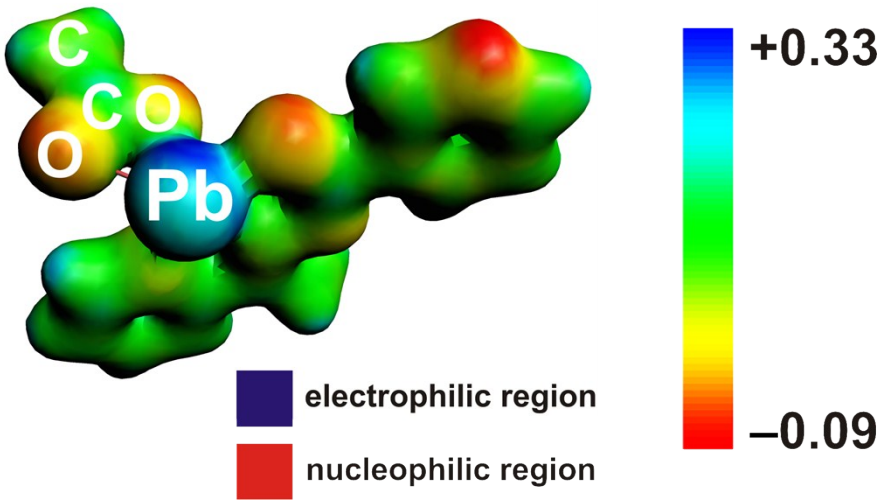

Fig. S1 The molecular electrostatic potential (DFT/BLYP-D3/ZORA/TZP) for the [PbL(OAc)] unit.

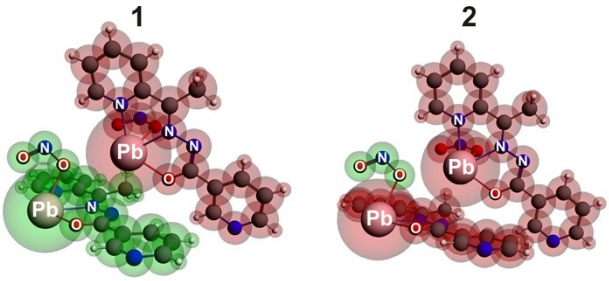

	$\pi\cdots\pi$/$Pb^{II}\cdots$N/$Pb^{II}\cdots$O (1)	$Pb^{II}\cdots NO_2^-$ (2)
ΔE_{int}	–20.55	–144.06
ΔE_{elstat}	–18.38	–131.80
ΔE_{orb}	–9.07	–64.13
$\Delta E_{dispersion}$	–19.83	–7.66
ΔE_{Pauli}	26.74	59.54

$\Delta E_{int} = \Delta E_{elstat} + \Delta E_{orb} + \Delta E_{dispersion} + \Delta E_{Pauli}$

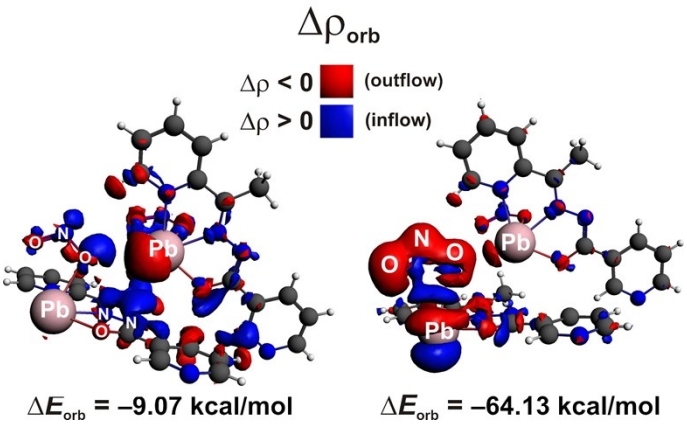

Fig. S2 (top) Cluster models of **[PbL(NO$_2$)]$_n$** together with the fragmentation patterns **1** and **2** applied in the ETS-NOCV analysis. (bottom) The overall deformation densities $\Delta\rho_{orb}$ of **1** and **2** with the corresponding energies ΔE_{orb}.

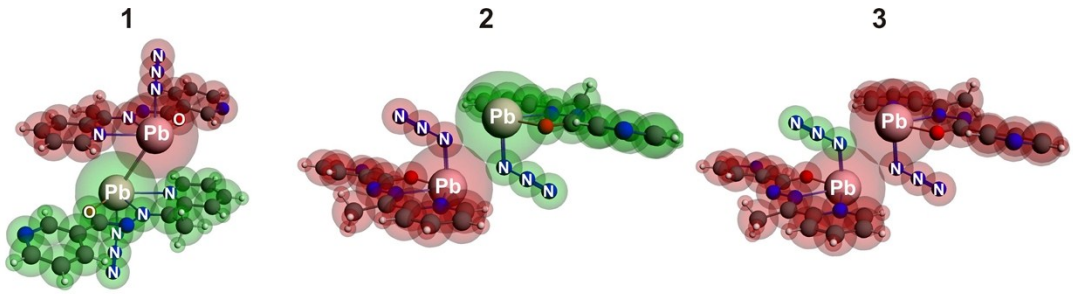

	$\pi\cdots\pi$/$Pb^{II}\cdots$N/$Pb^{II}\cdots Pb^{II}$ (1)	$Pb^{II}\cdots$N (2)	$Pb^{II}\cdots N_3^-$ (3)
ΔE_{int}	–15.86	–22.00	–129.56
ΔE_{elstat}	–9.78	–35.57	–165.23
ΔE_{orb}	–6.03	–14.66	–71.11
$\Delta E_{dispersion}$	–20.87	–10.76	–9.48
ΔE_{Pauli}	20.82	38.99	116.26

$\Delta E_{int} = \Delta E_{elstat} + \Delta E_{orb} + \Delta E_{dispersion} + \Delta E_{Pauli}$

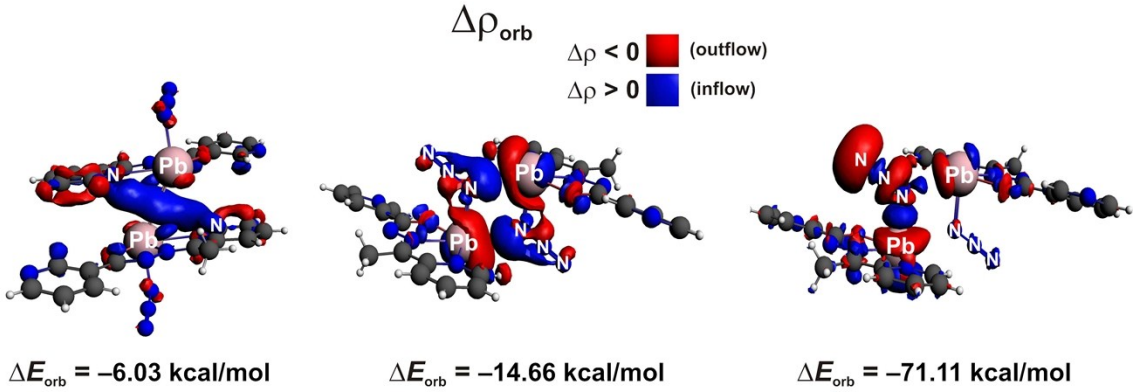

ΔE_{orb} = –6.03 kcal/mol | ΔE_{orb} = –14.66 kcal/mol | ΔE_{orb} = –71.11 kcal/mol

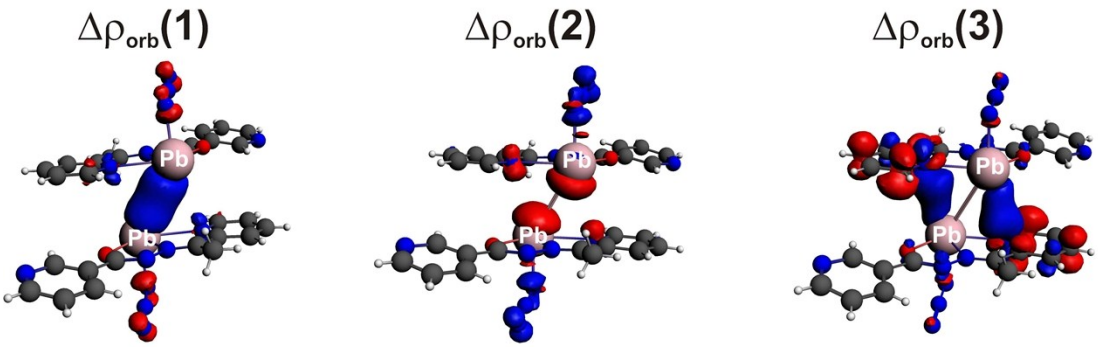

$\Delta E_{orb}(1)$ = –1.3 kcal/mol | $\Delta E_{orb}(2)$ = –0.7 kcal/mol | $\Delta E_{orb}(3)$ = –0.5 kcal/mol

Fig. S3 (top) Cluster models of **$[PbLN_3]_n$** together with the fragmentation patterns **1–3** applied in the ETS-NOCV analysis. (middle) The overall deformation densities $\Delta\rho_{orb}$ of **1–3** with the corresponding energies ΔE_{orb}. (bottom) The main NOCV-formation densities $\Delta\rho_{orb}(1–3)$ with the corresponding energies $\Delta E_{orb}(1–3)$ depicted for the bonding pattern **1**.

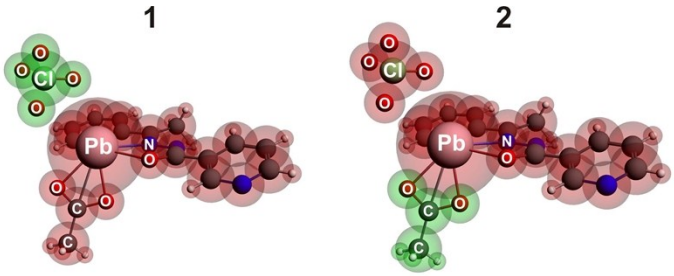

	$Pb^{II}\cdots ClO_4^-$ (1)	$Pb^{II}\cdots OAc^-$ (2)
ΔE_{int}	–74.53	–144.07
ΔE_{elstat}	–68.11	–176.73
ΔE_{orb}	–12.55	–75.54
$\Delta E_{dispersion}$	–6.36	–5.20
ΔE_{Pauli}	12.48	113.40

$\Delta E_{int} = \Delta E_{elstat} + \Delta E_{orb} + \Delta E_{dispersion} + \Delta E_{Pauli}$

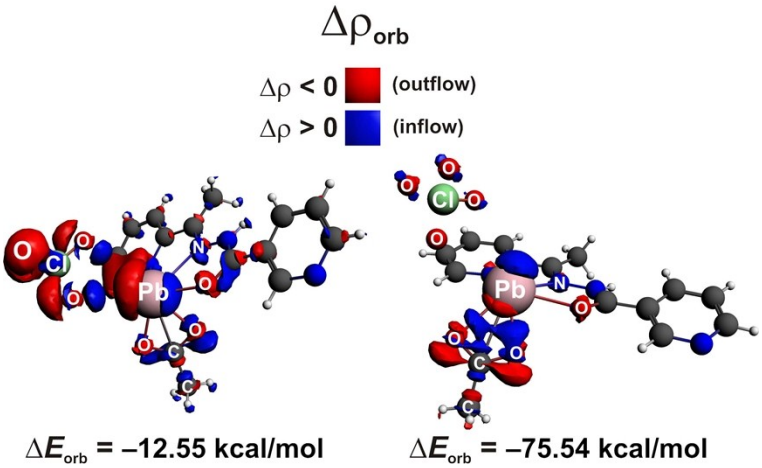

Fig. S4 (top) Cluster models of **{[Pb(HL)(OAc)]ClO_4}$_n$** together with the fragmentation patterns **1** and **2** applied in the ETS-NOCV analysis. (bottom) The overall deformation densities $\Delta\rho_{orb}$ of **1** and **2** with the corresponding energies ΔE_{orb}.

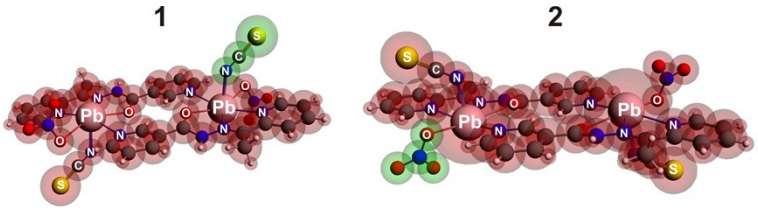

	$Pb^{II}\cdots NCS^{-}$ (1)	$Pb^{II}\cdots NO_3^{-}$ (2)
ΔE_{int}	–96.54	–96.87
ΔE_{elstat}	–101.75	–94.46
ΔE_{orb}	–52.15	–33.76
$\Delta E_{dispersion}$	–7.43	–6.86
ΔE_{Pauli}	64.80	38.21

$\Delta E_{int} = \Delta E_{elstat} + \Delta E_{orb} + \Delta E_{dispersion} + \Delta E_{Pauli}$

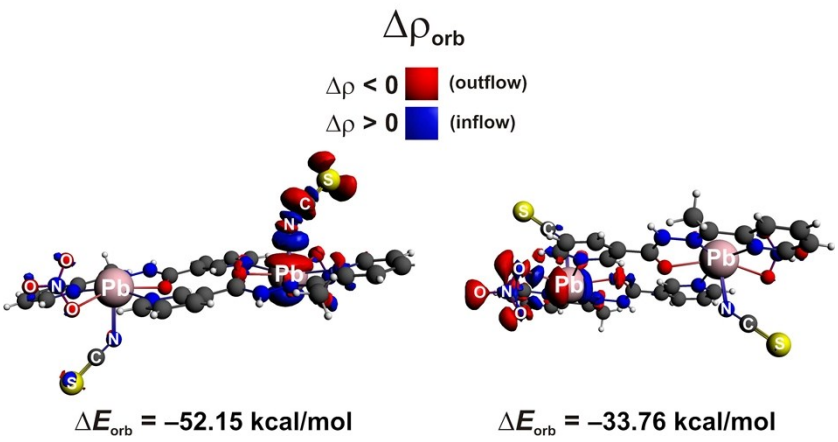

ΔE_{orb} = –52.15 kcal/mol ΔE_{orb} = –33.76 kcal/mol

Fig. S5 (top) Cluster models of **$[Pb_2(HL)_2(NO_3)_2(NCS)_2]$** together with the fragmentation patterns **1** and **2** applied in the ETS-NOCV analysis. (bottom) The overall deformation densities $\Delta\rho_{orb}$ of **1** and **2** with the corresponding energies ΔE_{orb}.

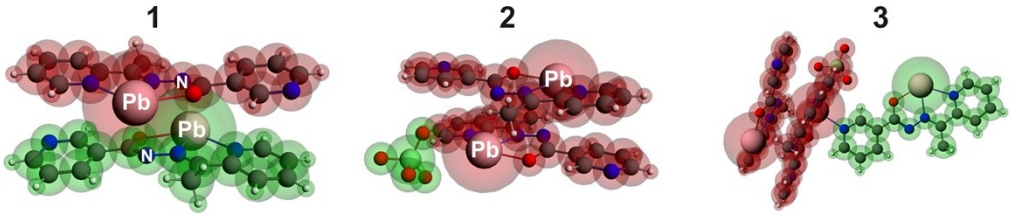

	$\pi\cdots\pi$/$Pb^{II}\cdots$N (1)	$Pb^{II}\cdots ClO_4^-$ (2)	$Pb^{II}\cdots$L (3)
ΔE_{int}	–11.31	–126.66	–6.15
ΔE_{elstat}	12.99	–111.42	–28.00
ΔE_{orb}	–37.07	–19.49	–30.23
$\Delta E_{dispersion}$	–41.89	–7.43	–11.70
ΔE_{Pauli}	54.66	11.68	63.78

$\Delta E_{int} = \Delta E_{elstat} + \Delta E_{orb} + \Delta E_{dispersion} + \Delta E_{Pauli}$

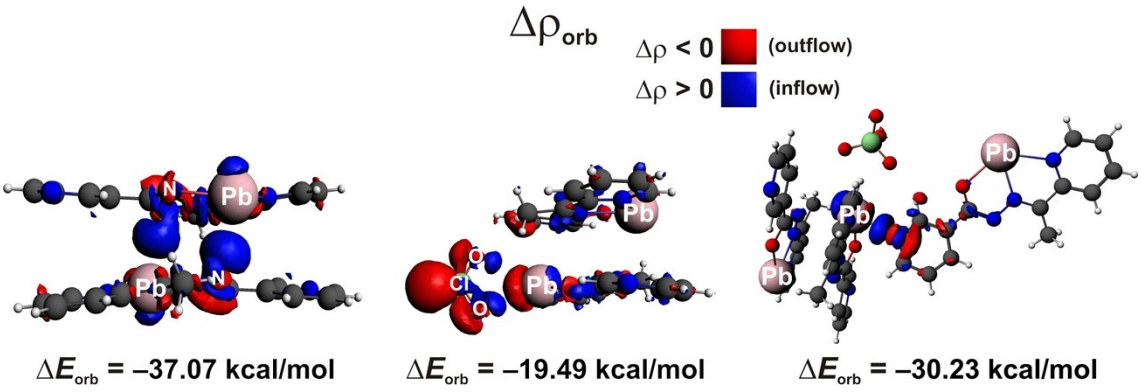

ΔE_{orb} = –37.07 kcal/mol ΔE_{orb} = –19.49 kcal/mol ΔE_{orb} = –30.23 kcal/mol

Fig. S6 (top) Cluster models of **{[PbL]ClO_4}$_n$·nH_2O** together with the fragmentation patterns **1–3** applied in the ETS-NOCV analysis. (bottom) The overall deformation densities $\Delta\rho_{orb}$ of **1–3** with the corresponding energies ΔE_{orb}.

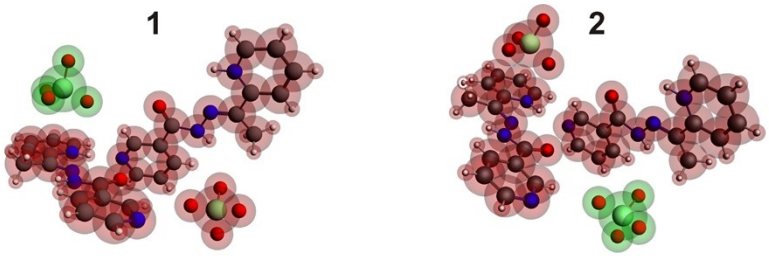

	$[H_2L]^+\cdots ClO_4^-$ (1)	$[H_2L]^+\cdots ClO_4^-$ (2)
ΔE_{int}	–69.43	–67.40
ΔE_{elstat}	–56.91	–56.76
ΔE_{orb}	–10.67	–12.81
$\Delta E_{dispersion}$	–6.66	–6.56
ΔE_{Pauli}	4.82	8.73

$\Delta E_{int} = \Delta E_{elstat} + \Delta E_{orb} + \Delta E_{dispersion} + \Delta E_{Pauli}$

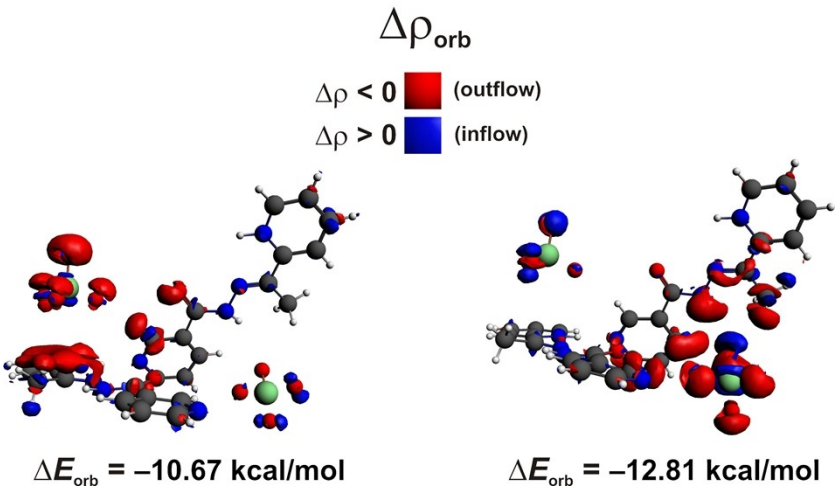

ΔE_{orb} = –10.67 kcal/mol ΔE_{orb} = –12.81 kcal/mol

Fig. S7 (top) Cluster models of **$[H_2L]ClO_4$** together with the fragmentation patterns **1** and **2** applied in the ETS-NOCV analysis. (bottom) The overall deformation densities $\Delta\rho_{orb}$ of **1** and **2** with the corresponding energies ΔE_{orb}.